ISSN 2079-1704. Хімія, фізика та технологія поверхні. 2025. Т. 16. № 3. С. 348-359

PACS 81.20.Ka; 64.70.Nd; 81.07.-b doi: 10.15407/hftp16.03.348

T.F. Lobunets [1], O.V. Shyrokov [1], O.A. Korniienko [1], Yu.V. Yurchenko [1], T.V. Tomila [1], A.V. Ragulya [1, 2]

STRUCTURE FORMATION OF NANOPOWDERS OF COMPLEX OXIDE PHASES OF $LaLuO_3$:Yb^{3+} PEROVSKITE TYPE BY THE PECHINI COMPLEXING CITRATE METHOD

[1] Frantsevich Institute for Problems of Materials Science of National Academy of Sciences of Ukraine
3 Omeliana Pritsaka Str., Kyiv, 03142, Ukraine, E-mail: shyrokovav@gmail.com
[2] National Technical University of Ukraine "Igor Sikorsky Kyiv Polytechnic Institute"
37 Beresteysky Avenue, Kyiv, 03056, Ukraine

The synthesis of nanopowders is of significant importance in the development of new materials. The sol-gel method is one of the simplest methods for the synthesis of unstable precursors, the thermal decomposition of which allows for the production of nanodispersed powders. The objective of this study was to examine the thermal decomposition of a precursor synthesized by the citrate method of polymer complexes, with the aim of obtaining nanopowders of perovskite-type complex oxide phases in the La_2O_3-Lu_2O_3-Yb_2O_3 system as one of the important stages in the creation of materials with specified characteristics. The study of the thermal decomposition of the precursor revealed that the destruction of the polymer matrix in the temperature range of 180–750 °C is accompanied by the formation of an X-ray amorphous intermediate. Upon further heating to 800–820 °C, this intermediate crystallizes with negligible decomposition (according to XRD) into perovskite of orthorhombic syngony with lattice parameters a = 0.6016 nm, b = 0.8390 nm, c = 0.5821 nm and density γ_{xrd} = 8.18 g/cm^3, and capillary-slit pore structure, with a specific surface area of 12–17 m^2/g, which corresponds to a particle size of 40–60 nm. The thermal decomposition of the precursor occurs through the storage and formation of a non-rigid component of the pore structure of intermediate metastable amorphous products before the formation of the perovskite phase in the La_2O_3-Lu_2O_3-Yb_2O_3 system at the temperature of 750 °C. The dependence of the general porosity characteristics of the studied samples on temperature during the non-isothermal decomposition of the precursor synthesized by the citrate method is not monotonic, with inflection points at 750 and 800 °C. At the temperature of 750 °C, the system undergoes a collapse, accompanied by a sharp decrease in the volume and specific surface area of mesopores. This is concomitant with the disappearance of the non-rigid component of the pore structure of intermediate amorphous products, as evidenced by a ledge on their nitrogen sorption isotherms. This signifies the completion of the thermal decomposition of polymeric complexes and the subsequent formation of perovskite-type complex oxide phases in the La_2O_3-Lu_2O_3-Yb_2O_3 system by nucleation, self-assembly, self-organization, and crystallization. An increase in the percentage of ytterbium dopant from 1 to 4 % does not affect significantly the general characteristics of the porous structure of perovskite samples; however, it does result in changes to their morphology. At the concentration of 4 % Yb^{3+}, the perovskite structure consists of particles of uniform morphology.

***Keywords**: precursors, Pechini (citrate) method, specific surface, nanopowders, $LaLuO_3$ perovskite, sorption isotherms*

INTRODUCTION

Materials with perovskite-type structures and the general formula ABO_3 are a diverse class of materials. In the 1960s, the authors [1, 2] first described compounds containing two different rare earth elements $LnLn'O_3$ in their structure. Since then, interest of scientific community in these materials has grown due to their physical and chemical properties. These compounds are suitable as electrolytes for electrochemical devices, such as solid oxide fuel cells (SOFCs), electrolyzers, sensors, hydrogen separation membranes, and electrochemical catalytic reactors [3–5] due to their high ionic conductivity and low activation energy. Additionally, $LaLuO_3$-based materials are being considered as replacements for silica (κ = 3.9) as the primary gate dielectric owing to their high κ value (above 40) [6].

Lanthanum oxide-based materials are known to hydrate when exposed to air, forming lanthanum hydroxide structures. This transition can lead to sample destruction, which is undesirable for material fabrication. Previous studies [3, 7–9] have investigated the stability of the ordered phase with a perovskite-type structure of $LaLnO_3$, which

contains a significant number of La^{3+} ions, in aggressive environments. The chemical resistance of materials with an ordered structure, such as perovskite containing lanthanum, was confirmed in terms of interaction with gas atmosphere components in studies of compositions $La_{1-x}M_xYbO_{3-\delta}$ (M = Ca, Sr, Ba; x = 0, 0.05, 0.1) [3, 9], $La_{0.9}Sr_{0.1}YO_{3-\delta}$ [7], $La_{0.95}Ca_{0.05}ScO_{3-\alpha}$, and $La_{0.9}Sr_{0.1}ScO_{3-\alpha}$ [8]. The chemical stability of $La_{0.9}Ba_{0.1}YbO_{3-\delta}$ was investigated in CO_2 (pCO_2 = 1 atm) and H_2O (20 % H_2O-Ar) atmospheres at various temperatures (200, 400, 600, and 800 °C) for 24 hours [9]. The material remained single-phase, as evidenced by the absence of additional diffraction peaks in the XRD data. Thus, it can be concluded that an ordered phase $LaMO_3$ with a perovskite-type structure containing lanthanum ions can provide a chemically stable phase without decomposition in the presence of CO_2 and H_2O.

In [10], the temperatures required for the formation of an ordered structure, such as $LaLn'O_3$ perovskite, depending on the Ln/Ln' ratio, were determined. For instance, the formation temperature of $LaLuO_3$ perovskite is 830 °C, whereas that of $LaYbO_3$ perovskite is ~ 880 °C. Therefore, when creating a $LaLuO_3$:Yb^{3+} material, an increase in the concentration of Yb^{3+} ions in the $LaLuO_3$ crystal lattice is likely to increase the ordering temperature of this phase from 830 to ~ 880 °C.

State diagrams of multicomponent systems allow the selection of optimal compositions for the creation of new materials [11–13]. Information regarding the layout of the state diagrams of multicomponent oxide systems can be used to determine the concentration and temperature limits for the existence of an ordered phase with a perovskite-type structure. The phase equilibria in the three-component La_2O_3-Lu_2O_3-Yb_2O_3 system have been studied in [11, 12]. The authors have found that in this system, along with the isoconcentrate of 50 mol. % La_2O_3, a continuous series of solid solutions is formed based on an ordered phase with a perovskite-type structure, which makes it possible to vary the amount of Yb^{3+} dopant.

The synthesis method used to create the nanopowders is essential for the creation of new materials. The desired properties can be achieved using different synthesis routes. The sol-gel method is a simple approach for synthesizing unstable precursors, which can then be thermally decomposed to produce nanodispersed powders. This method offers several advantages over other synthesis methods, including control over the material size and surface properties, ease of implementation, high quality, and production of materials with a large surface area [14–16]. The polymer complex method (citrate method) is one of the most commonly used sol-gel methods. This method involves the formation of chelate complexes between alpha-hydroxy acids (citric acid) and metal ions, which are then heated to 100–140 °C in the presence of multifunctional alcohols (ethylene glycol). Low molecular weight oligomers are created, which, upon further heating through polycondensation, form a polymer gel with evenly spaced metal atoms. The thermal decomposition of this gel allows the production of materials with a high degree of homogeneity and dispersion. This is achieved through careful control of the ratio of the components, duration, and temperature of polymerization.

This study examines the thermal decomposition of a precursor synthesized using the citrate method, which is a crucial step in creating materials with specific characteristics.

MATERIALS AND METHOD

This study analyzed samples of non-isothermal decomposition of precursors synthesized by the citrate (polymer gel) method. These include intermediate samples obtained at different decomposition temperatures and the final $LaLuO_3$ perovskites doped with ytterbium. The following reagents were used for precursor synthesis: La_2O_3, Lu_2O_3, and HNO_3 (puriss. spec.), citric acid (p.a.), and NH_4OH. These were in the form of 0.5 M solutions of $La(NO_3)_3$ and $Lu(NO_3)_3$ and $Yb(NO_3)_3$, 1 M citric acid solution, and 25 % NH_4OH solution. The nitrate solutions were mixed with ethylene glycol and citric acid solution at approximately 90 °C under intense stirring. After a certain period of time, a 25 % solution of NH_4OH was gradually added and stirring was continued while maintaining the temperature for 15–20 minutes. The resulting solutions were dried in an oven for 24 hours at a temperature of 120–250 °C.

To study the evolution of the structure during the formation of complex oxide phases, such as perovskite, we used samples from the intermediate and final thermal decomposition of precursor S1 (1 % Yb^{3+}), dried at temperatures

ranging from 120–250 °C. Precursor S4 (4 % Yb^{3+}), with an increased yttrium content and the drying temperature of 120 °C, was used to study the effect of yttrium content on the formation of complex oxide phases, such as perovskite, by non-isothermal decomposition at a constant rate.

The intermediate and final nanopowders of complex oxide phases, such as perovskite, in the La_2O_3-Lu_2O_3-Yb_2O_3 system, obtained by the thermal decomposition of the precursor, were studied using physicochemical methods, including thermogravimetric analysis, X-ray diffraction (XRD), adsorption-structural method, and electron microscopy.

Thermogravimetric analysis was performed using a DQ-1000 derivatograph. Powder diffraction method was used to obtain the diffraction patterns of the samples using a SmartLab SE multifunctional laboratory X-ray diffractometer. The SmartLab Studio II software package was used to process the data and determine the phase composition and structural characteristics of the samples. Infrared spectra were studied using a FTIR spectrometer FSM-1201 in the wavelength range of 4000–400 cm^{-1}. To measure the samples, they were mixed with KBr powder in a ratio of 1:300 milligrams and the resulting mixture was pressed into transparent tablets with a diameter of 13 mm. The porous structure of the obtained samples was investigated using the adsorption-structural static volumetric method on an ASAP 2000M (Accelerated Surface Area and Porosimetry System) instrument, which was designed to obtain gas adsorption isotherms. The isotherms are interpreted to calculate the total pore volume (V_{sum}, cm^3/g) and specific surface area S_{BET} m^2/g using the BET method (Brunauer S., Emmett P.H., Teller E.), total volume (V_{me}, cm^3/g) and surface area (S_{me}, m^2/g) of mesopores, total volume (V_{me}, cm^3/g) and surface area (S_{me}, m^2/g) of micropores and external surface area (S_{exter}, m^2/g) according to the t-method, as well as differential distributions of mesopore volume and surface area calculated according to the theory of Barrett E.P., Joyner L.S., Halenda P.P. (BJH). Nitrogen was used as the sorbing gas. The measurement range of this method is within the equivalent pore size range of 0.3 to 300 nm.

RESULTS AND DISCUSSION

Thermogravimetric analysis. The temperatures for obtaining the intermediate samples were selected based on the thermal decomposition of the synthesis precursor S1. Based on derivatographic studies, the polymer complex synthesized by the citrate method with the citrate molecules of REE included in it undergoes thermal decomposition in multiple stages (Fig. 1). This process is accompanied by endothermic effects up to 180 °C and exothermic effects in the temperature range 180-675 °C. These effects are associated with the drying and destruction of the polymer matrix, leading to the formation of an X-ray amorphous oxide or carbonate precursor, or both at once. Primary mass loss occurs during these stages, amounting to approximately 27 %. At temperatures above 750 °C, another exothermic effect is observed, accompanied by a slight mass loss. This may be due to the destruction of the remnants of the oxide-carbonate precursor, ordering and formation of perovskite phase grain nuclei, their self-assembly and self-organization, and crystallization. Thus, to study the evolution of the structure of nanopowders in the preparation of complex oxide phases such as perovskite in the La_2O_3-Lu_2O_3-Yb_2O_3 system, according to the derivatographic data of the synthesized precursor S1, the temperatures for obtaining intermediate and final samples under non-isothermal decomposition with a heating rate of 5 °C/min were initially 250, 300, 400, 475, 575, 675, 700, 750, 800, and 825 °C.

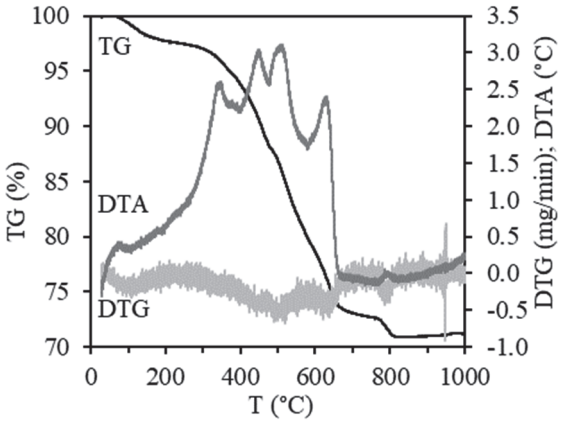

Fig. 1. Derivatographic studies of the non-isothermal decomposition of the precursor synthesized by the citrate method (synthesis S1)

Nanopowders in the La_2O_3-Lu_2O_3-Yb_2O_3 system with a high ytterbium content were obtained at the temperature of 825 °C, as determined by derivatographic studies of the thermal decomposition of polymer complex S4 synthesized by the citrate method.

Infrared spectroscopy. Infrared spectroscopic studies were conducted on the thermally decomposed samples of the synthesized precursors in the wavelength range of 4000–450 cm^{-1}. The spectra of the initial precursor sample (synthesis S1), obtained at a temperature of 120–250 °C, showed a set of absorption bands in the frequency range of ν ~ 800–450 cm^{-1}, characterizing M-O vibrations, where M = La, Lu (Fig. 2 *a*). In the frequency range of ν ~ 1110–845 cm^{-1} the absorption bands of valence C-O vibrations can be observed. The absorption bands in the frequency range of ν ~ 1600–1150 cm^{-1} characterize the vibrations of COO^- carbonate ions in different coordination (monodentate and bidentate) [17–20].

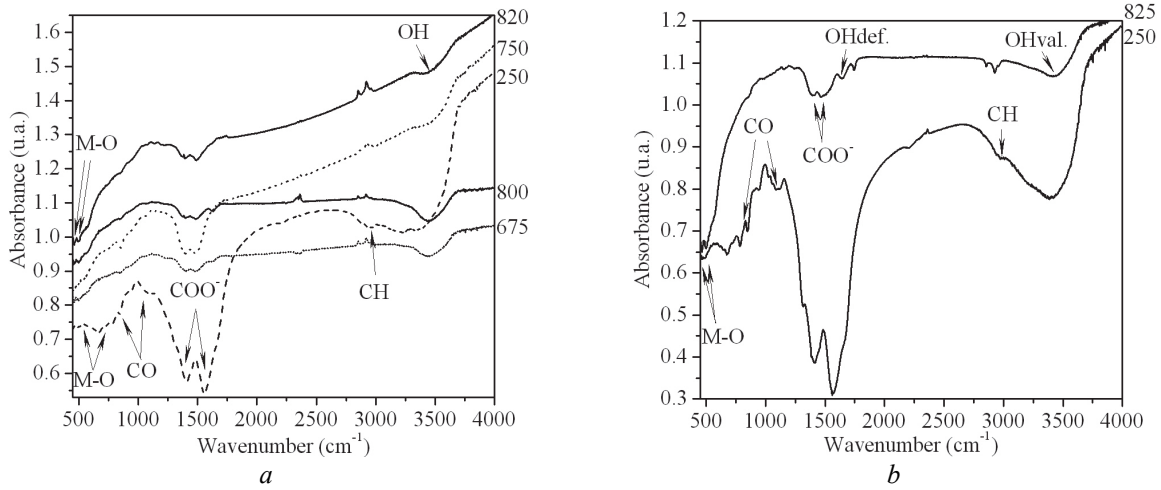

Fig. 2. Infrared spectra of samples from the non-isothermal decomposition at temperatures 250–820 °C of precursors synthesized by the citrate method: *a* – S1, *b* – S4

The thermal decomposition of precursor S1 under non-isothermal conditions up to 675 °C is accompanied by a decrease in the intensity of the absorption bands in the IR spectrum of carbonate ions. Additionally, new absorption bands with frequencies of approximately 470 and 503 cm^{-1} appear. These changes indicate further decomposition of the polymer complex and the formation of amorphous nuclei for self-assembly and self-organization of the $LaLuO_3$ perovskite structure. As the temperature increases, the intensity of the peaks increases and the absorption band narrows, indicating the formation of a $LaLuO_3$ perovskite-type structure. Furthermore, a decrease in carbonate ion absorption band intensity is observed in the 675–820 °C temperature range (Fig. 2 *a*). However, weak carbonate bands are also present in the samples synthesized at 820 °C. Although lanthanide oxides have a strong tendency to absorb water and carbon dioxide, resulting in the observation of OH and carbonate group absorption peaks in the infrared spectra of these compounds [19], the ordered phase with a perovskite-type structure containing $LaMO_3$ lanthanum ions exhibits high chemical stability in the presence of CO_2 and H_2O. The weak carbonate bands present in the IR spectra of the final samples are likely a result of the extended processes of self-organization, self-assembly, and the formation of perovskite-type particles during thermal decomposition under non-isothermal conditions. This leads to the agglomeration of the synthesized product. It is important to note that the IR spectroscopic studies of the thermal decomposition samples of the synthesized precursors under different conditions of polymer complex synthesis are similar. Therefore, the IR spectra of the thermal decomposition samples of the synthesis precursors S1 and S4 are identical (see Fig. 2 *b*).

XRD analysis. XRD studies were conducted on the intermediate and final samples of non-isothermal decomposition of precursor S1, which was synthesized by the citrate method, to investigate the structure formation of complex oxide phases such as perovskite in the La_2O_3-Lu_2O_3-Yb_2O_3 system (refer to Figs. 3 and 4). The results showed that the structural evolution process occurs mainly in two stages: decomposition of the polymer complex formed

during precursor synthesis and formation of the perovskite phase. The X-ray-amorphous structure of the intermediate samples of non-isothermal decomposition remains up to a decomposition temperature of 700 °C. The initial formation stage of the perovskite phase commences at a decomposition temperature of 750 °C, as evidenced by the emergence of peaks that correspond to the crystallographic planes (1 2 1) and (2 0 2) of the $LaLuO_3$ perovskite. Formation process of the perovskite phase under these conditions is completed at 820 °C. Table 1 presents the phase composition and structural parameters of the intermediate and final samples obtained from the non-isothermal decomposition of precursor S1.

Table 1. Phase composition and structural parameters of the samples from non-isothermal decomposition of precursor S1 with respect to temperature

Temperature °C	Phase composition phase	wt.%	Crystallinity %	*a* nm	*b* nm	*c* nm	*V* Å^3	*L* nm	γ_{xrd} g/cm^3
800	amorphous	1.6							
	perovskite	98.4	94.7	0.6020	0.8398	0.5824	294.5	59.7	8.16
820	perovskite	100	100	0.6016	0.8390	0.5821	293.8	63.7	8.18

a, *b*, *c* – unit cell parameters; *V* – unit cell volume; *L* – crystallite size; γ_{xrd} – sample density calculated from X-ray diffraction data

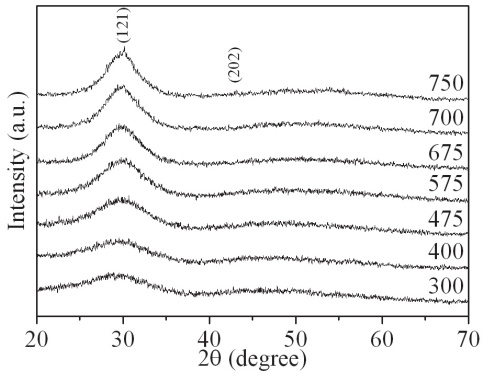

Fig. 3. X-ray diffraction studies of the structural evolution of samples of the non-isothermal decomposition of precursor S1 in relation to the temperature

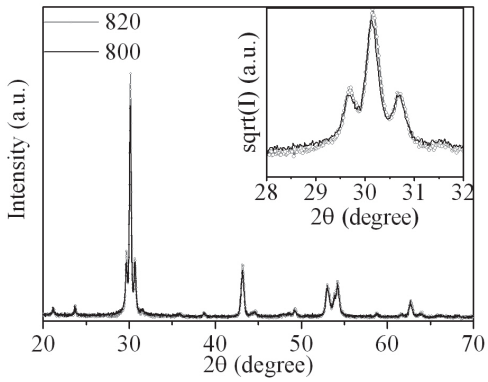

Fig. 4. Diffraction patterns of the final thermal decomposition products at 800 °C. The inset shows an elevated background at 800 °C compared to 820 °C

The increased content of ytterbium in the precursor (synthesis S4), when perovskites are obtained by thermal decomposition under non-isothermal conditions at a rate of 5 °C/min, does not significantly affect the structural parameters. Thus, the lattice parameters of the samples vary by ~ 0.15% that of S1.

Adsorption-structural studies of the pore structure evolution during thermal decomposition. As the polymer complex decomposes, its porous structure changes and, as shown by the adsorption-structural method, the appearance of hysteresis loops changes in the nitrogen sorption isotherms obtained for the samples studied. Thus, the nitrogen sorption isotherms of the intermediate and final samples of the non-isothermal decomposition of the precursor synthesized by the citrate method to obtain ytterbium-doped perovskite $LaLuO_3$:Yb^{3+} belong to type IV isotherms according to the Brunauer, Deming, Deming, and Teller (BDDT) classification, which characterizes them as mesoporous nanodispersed bodies (Fig. 5) [21]. According to the IUPAC classification, the hysteresis loops in the isotherms of the samples belong to the H3 type, indicating a slit-like pore structure [22]. It should be noted that in the structure of intermediate metastable products, during decomposition, pores appear between parallel layers of supramolecular structures that are not rigidly bound to each other ("non-rigid component of the structure" of the sample), which has a characteristic type of hysteresis loops and is recorded as a ledge on their nitrogen sorption isotherms [23, 24]. This allows the temperature range of its existence and degradation to be determined. Its occurrence is due to the sequential destruction of the initial coordination bonds of the polymer complex during the detachment of H_2O, CO, CO_2, and NO molecules and the formation of new coordination bonds in the intermediate metastable products. The precursor synthesized under these conditions (S1 1 % Yb^{3+}) has a homogeneous pore structure with a non-rigid component; approximately 30 % of the mesopore surface is composed of pores with a size of 3.56 nm, which is typical for oxycarbonate phases (Fig. 5) [25–27]. The thermal decomposition of the synthesized precursor proceeds through the formation of intermediate metastable products of a layered structure with a non-rigid component up to 750 °C, while its amount gradually decreases. It should be noted that the dependence of the general porosity characteristics of the samples studied on the temperature during the non-isothermal decomposition of the precursor synthesized by the citrate method is not monotonic, with points of intersection at 750 and 800 °C (Fig. 6). At the temperature of 750 °C, the non-rigid component of the pore structure disappears, collapse of the system is observed, the volume of mesopores and the specific surface area decrease sharply, and differential curves of the volume and surface area distribution of mesopores by size indicate the formation of a metastable intermediate product of homogeneous porous structure with a mesopore size of predominantly 4.41 nm. The disappearance of the non-rigid component of the pore structure of the amorphous intermediate products indicates the end of the thermal decomposition of the polymeric complexes synthesized by the citrate method and the beginning of further nucleation, assembly, and growth of nanodispersed particles of complex oxide phases, such as perovskite, by predominantly self-assembly and self-organization. Increasing the temperature to 820 °C during the non-isothermal decomposition of the precursor obtained under these conditions leads to the formation of nanodispersed mesoporous powders with a capillary-slit pore structure with a trimodal distribution of mesopore sizes, and a specific surface area of 12–17 m^2/g, corresponding to a particle size of 40–60 nm.

Thus, the structure of the polymer complex synthesized under these conditions (by the citrate method) (synthesis S1) has a non-rigid component of the pore structure, which is preserved and formed in intermediate amorphous products throughout the thermal decomposition, until the system collapses at the temperature of 750 °C, and the formation of a perovskite-type phase in the La_2O_3-Lu_2O_3-Yb_2O_3 system begins. A further increase in temperature to 820 °C leads to the completion of formation of nanodispersed mesoporous powders with a capillary layer pore structure and a specific surface area of 12–17 m^2/g, corresponding to a particle size of 40–60 nm.

It should be noted that the pore structure of undoped $LaLuO_3$ perovskite samples obtained by thermal decomposition of precursors at the temperature of 850 °C and prolonged dwell time may consist of rigid lamellar particles or have a layered expansion lattice. As shown by adsorption-structural studies, the isotherm of the undoped perovskite sample has a low-pressure hysteresis loop type. This suggests that the thermal decomposition of the precursor may result in the formation of large agglomerates with a highly defective surface, a layered structure, and molecular entrances to the pores. The average diameter of the resulting particles, as determined

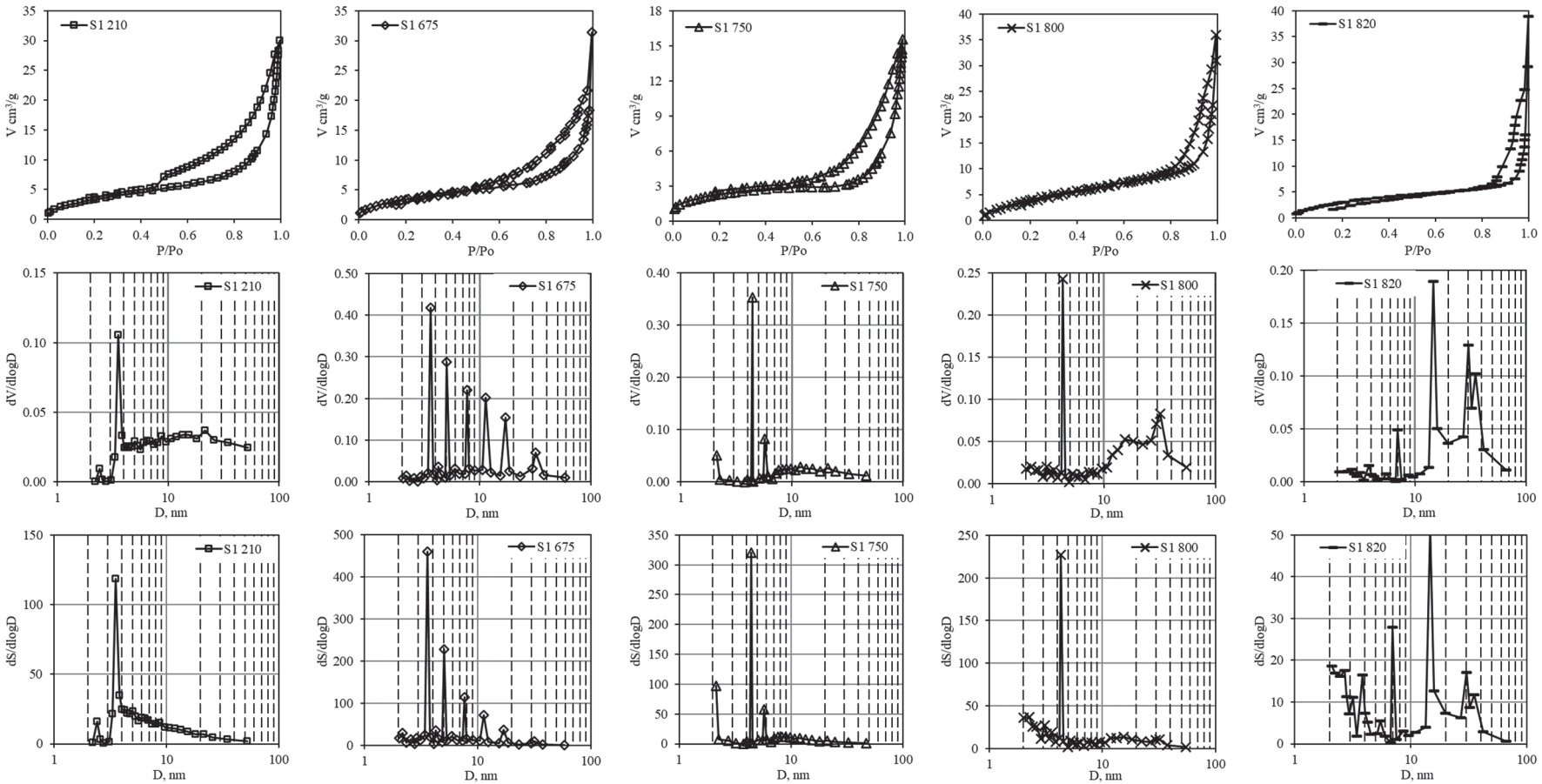

Fig. 5. Nitrogen sorption isotherms and differential distributions of mesopore volumes and surface areas by size on intermediate (*a–d*) and final (*e*) samples under non-isothermal decomposition of precursor S1

by the specific surface area of S_{BET}, is 63 nm (Fig. 7, Table 2). The incorporation of the doping additive, yttrium, results alterations in the sorption isotherms of the obtained samples, shifting to type IV, and leading to the removal of low pressure hysteresis.

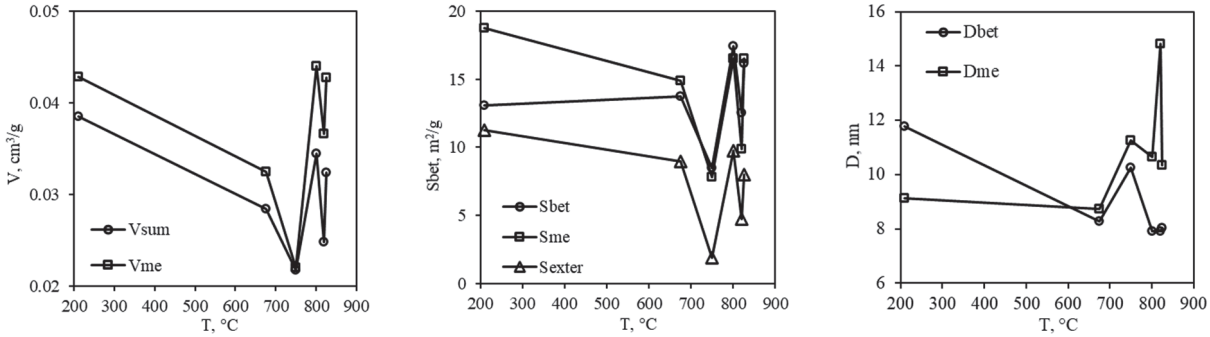

a *b* *c*

Fig. 6. Dependence of the general porosity characteristics of the intermediate and final samples on temperature for the non-isothermal decomposition of precursor S1

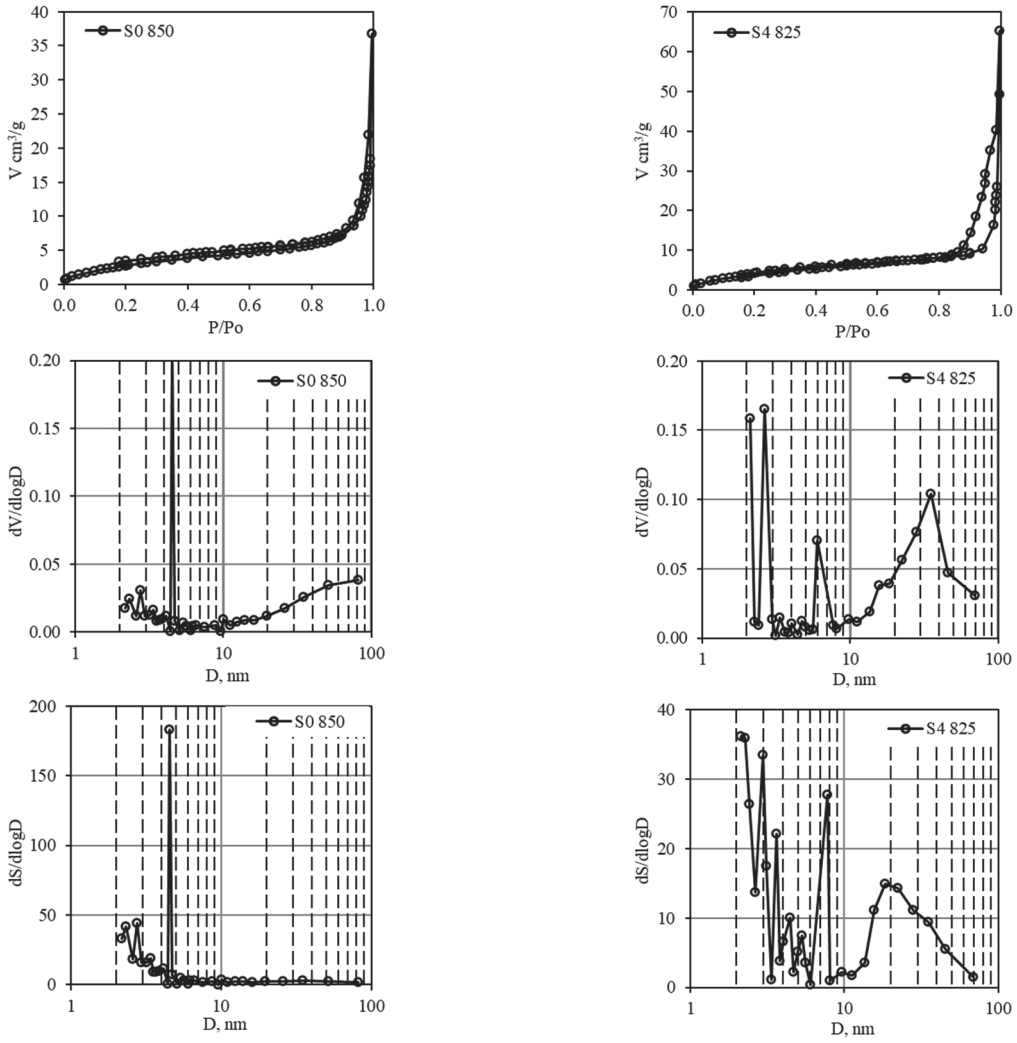

a *b*

Fig. 7. Nitrogen sorption isotherms and differential distributions of mesopore volumes and surface areas by size for non-isothermal decomposition of undoped S0 ($LaLuO_3$) and doped S4 ($LaLuO_3$:Yb^{3+}) precursor

Table 2. General characteristics of the pore structure of the obtained samples of complex oxide phases, such as perovskite in the La_2O_3-Lu_2O_3-Yb_2O_3 system

Sample	Temperature	V_Σ	BET		BJH desorption		
			S_{BET}	D_{BET} particle	V_{me}	S_{me}	$D_{av\ me}$
	°C	cm^3/g	m^2/g	nm	cm^3/g	m^2/g	nm
S0 0 % Yb^{3+}	850	0.0233	11.60	63.1	0.0334	10.50	12.8
S1 1 % Yb^{3+}	820	0.0248	12.55	58.3	0.0366	9.89	14.8
S4 4 % Yb^{3+}	825	0.0367	18.68	39.2	0.0605	14.15	17.1

When the percentage of the doping additive ytterbium is increased from 1 to 4% (synthesis S4), the type of isotherms of the obtained perovskite samples and the type of hysteresis loops remain unchanged and characterize them as nanodispersed mesoporous layered structures. The obtained samples also have a predominantly bi- and trimodal differential distribution of mesopore volumes and surfaces by size. Hence, the differential mesopore size distributions of perovskite samples obtained by the synthesis of precursor S1 show at least three mesopore size ranges with average equivalent diameters of 4, 16-17 and 34-45 nm with an average particle diameter of 60 nm (Figure 6). Increasing the percentage of ytterbium doping additive to 4% (syntheses S1 and S4) has a significant effect on the overall pore structure characteristics of the perovskite samples (Figure 7, Table 2).

Thus, the sample has a slightly increased pore volume and S_{BET} specific surface area, which characterize a particle size of 39 nm. At the same time, the external specific surface area S_{exter} calculated by the t-method has a higher value compared to the powder with 1 % Yb^{3+} of 4.7 and 6.1 m^2/g respectively, which also indicates a decrease in the particle size with increasing ytterbium content. In addition, the differential distribution of mesopore volumes and surfaces by size is bimodal. The wide distribution of mesopore volumes and surfaces by size indicates the presence of agglomerates of similar sizes. This is due to their morphology, which is confirmed by the SEM images of the studied samples (Figs. 8, 9). However, the image of the sample with 4 % ytterbium shows slightly larger particle sizes. They are also characterized by the uniformity of particles with clear boundaries that form a coral structure. The image with 1 % ytterbium shows smaller particle sizes but agglomerates forming a branched network structure. Thus, increasing the ytterbium content leads to the formation of nanostructured powders with different morphologies.

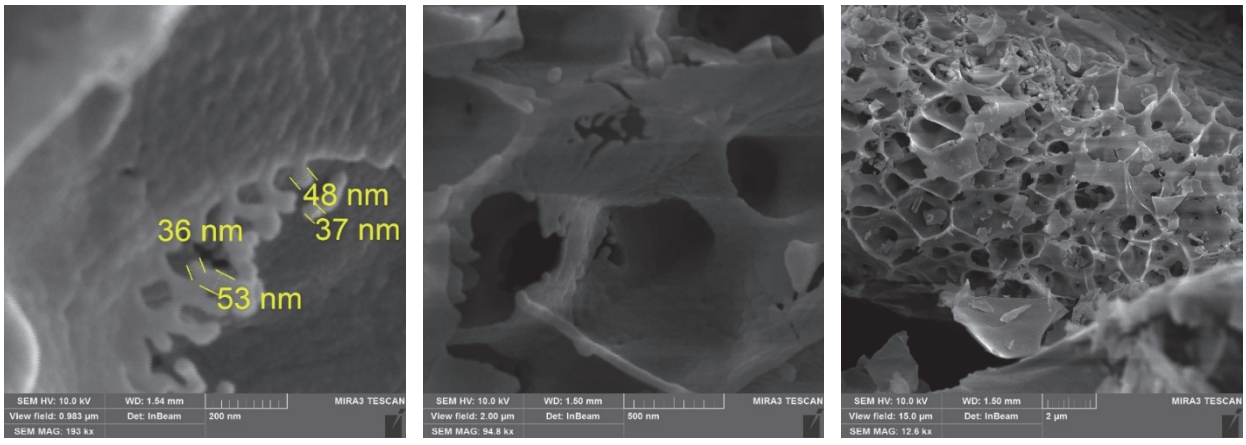

Fig. 8. SEM image of non-isothermal decomposition of precursor S1 after 820 °C

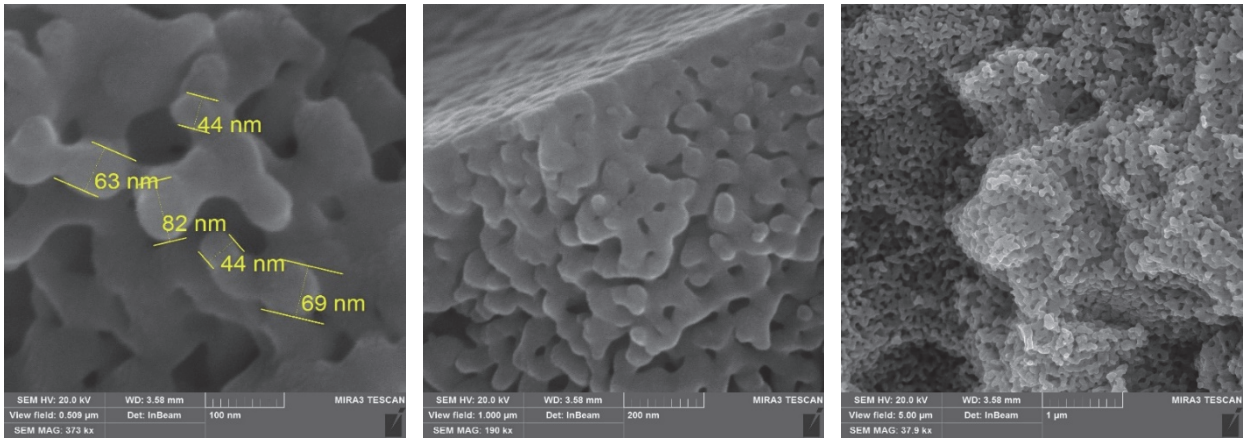

Fig. 9. SEM image of non-isothermal decomposition of precursor S4 after 825 °C

CONCLUSIONS

The thermal decomposition of polymeric complexes (precursors) synthesized by the citrate method to obtain complex oxide phases, such as perovskite, in the La_2O_3-Lu_2O_3-Yb_2O_3 system has been studied. It has been found that the destruction of the polymer matrix in the temperature range of 180-750 °C is accompanied by the formation of an X-ray amorphous intermediate which, upon further heating to 800–820 °C, crystallises with negligible decomposition according to XRD into perovskite of orthorhombic syngony with lattice parameters a = 0.6016 nm, b = 0.8390 nm, c = 0.5821 nm and density γ_{xrd} = 8.18 g/cm^3, with a specific surface area of 12–17 m^2/g, corresponding to a particle size of 40–60 nm. The thermal decomposition of the precursor proceeds through the storage and formation of a non-rigid component of the pore structure of the intermediate metastable amorphous products before the formation of the perovskite phase at the temperature of 750 °C. The dependence of the general porosity characteristics of the studied samples on temperature during the non-isothermal decomposition of the precursor synthesized by the citrate method is not monotonic, with intersections at 750 and 800 °C. At 750 °C, the system collapses, the volume and specific surface of the mesopores decrease sharply, and the non-rigid component of the pore structure of the intermediate amorphous products disappears, which is recorded as a ledge on their nitrogen sorption isotherms, indicating the completion of the thermal decomposition of polymeric complexes synthesized by the citrate method and the subsequent formation of complex oxide phases such as perovskite by nucleation, self-assembly, self-organization, and crystallization. Upon non-isothermal decomposition of the precursors synthesized under these conditions, the perovskite samples obtained have a predominantly bi- or trimodal distribution of mesopore sizes. At least three mesopore size ranges with average equivalent diameters of 4, 16–17 and 34–45 nm with an average particle diameter of 40–90 nm are observed in the differential mesopore size distributions of the perovskite samples, which is related to the morphology of the samples. An increase in the percentage of ytterbium doping additive from 1 to 4 % does not significantly affects the general characteristics of the porous structure of the perovskite samples and changes their morphology. At 4 % Yb^{3+}, the perovskite structure consists of particles of the same shape.

ACKNOWLEDGEMENTS

This work was supported by the NATO SPS MYP G5769 project “Laser Ceramics for Detector of Harmful Substances”.

Формування структури нанопорошків складних оксидних фаз $LaLuO_3:Yb^{3+}$ типу перовськіту, отриманих комплексоутворюючим цитратним методом Печіні

О.В. Широков, Т.Ф. Лобунець, О.А. Корнієнко, Ю.В. Юрченко, Т.В. Томіла, А.В. Рагуля

Інститут проблем матеріалознавства ім. І.М. Францевича Національної академії наук України
вул. Омеляна Пріцака, 3, Київ, 03142, Україна, shyrokovav@gmail.com
Національний технічний університет України «Київський політехнічний інститут імені Ігоря Сікорського»
пр-т Берестейський, 37, Київ, 03056, Україна

Важливу роль при створенні нових матеріалів відіграє метод синтезу нанопорошків. Золь-гель метод є одним із найпростіших методів синтезу нестійких прекурсорів, термічне розкладання яких дозволяє отримувати нанодисперсні порошки. Метою роботи було дослідження процесу термічного розкладання прекурсора, синтезованого цитратним методом полімерних комплексів, для отримання нанопорошків складних оксидних фаз типу перовськіту у системі La_2O_3-Lu_2O_3-Yb_2O_3 як однієї з важливих стадій створення матеріалів з заданими характеристиками. Дослідження термічного розкладання прекурсора показали, що руйнування полімерної матриці у діапазоні температур 180-750 °С супроводжується утворенням рентгеноаморфного проміжного продукту, який при подальшому нагріванні до 800-820 °С кристалізується з незначним розкладанням згідно РФА у перовськіт орторомбічної сингонії з періодами ґратки a = 0.6016 нм, b = 0.8390 нм, c = 0.5821 нм та густиною γ_{xrd} = 8.18 г/см^3, капілярно-щілинної порової будови, з питомою поверхнею 12–17 м^2/г, що відповідає розміру частинок 40–60 нм. Термічне розкладання прекурсора відбувається через зберігання та утворення нежорсткої складової порової будови проміжних метастабільних аморфних продуктів до початку формування фази перовськіту у системі La_2O_3-Lu_2O_3-Yb_2O_3 при 750 °С. Залежність загальних характеристик пористості досліджених зразків від температури при неізотермічному розкладанні синтезованого цитратним методом прекурсора має немонотонний характер з точками перегину при 750 та 800 °С. При 750 °С в системі виникає колапс, об'єм та площа питомої поверхні мезопор різко зменшуються, а зникнення нежорсткої складової порової будови проміжних аморфних продуктів, що фіксується у вигляді плеча на їхніх ізотермах сорбції азоту, свідчить про закінчення процесу термічного розкладання полімерних комплексів та подальше формування складних оксидних фаз типу перовськіту у системі La_2O_3-Lu_2O_3-Yb_2O_3 шляхом зародкоутворення, самоскладання і самоорганізації та кристалізації. Підвищення відсотку легуючої добавки ітербію з 1 до 4 % істотно не впливає на загальні характеристики пористої структури зразків перовскитів, але змінює їхню морфологію. При 4 % Yb^{3+} структура перовськіту складається із частинок однакової форми.

***Ключові слова**: прекурсори, метод Печіні (цитратний), питома поверхня, нанопорошки, перовськіт $LaLuO_3$, ізотерми сорбції*

REFERENCES

1. Schneider S.J., Roth R.S. Phase Equilibria in Systems Involving the Rare-Earth Oxides. Part II. Solid State Reactions in Trivalent Rare-Earth Oxide Systems. *Journal of Research of the National Bureau of Standards Section A: Physics and Chemistry.* 1960. **64A**(4): 317.
2. Meller-Buschbaum Von Hk., Graebne P.-H. Zur Krirtallstruktur von $LaErO_3$ und $LaLuO_3$. *Zeitschrift für anorganische und allgemeine Chemie.* 1971. **386**(2): 158.
3. Kasyanova A.V., Lyagaeva J.G., Vdovin G.K., Murashkina A.A., Medvedev D.A. Transport properties of $LaYbO_3$-based electrolytes doped with alkaline earth elements. *Electrochim. Acta.* 2023. **439**: 141702.
4. Zhang W., Hu Y.H. Progress in proton-conducting oxides as electrolytes for low-temperature solid oxide fuel cells: from materials to devices. *Energy Sci. Eng.* 2021. **9**(7): 984.
5. Boubchir M., Aourag H. Materials genome project: Mining the ionic conductivity in oxide perovskites. *Mater. Sci. Eng: B.* 2021. **267**: 114984.
6. Tryus M., Nikolaev K.V., Makhotkin I.A., Schubert Jü., Kibkalo L., Danylyuk S., Giglia A., Nicolosi P., Juschkin L. Optical and structural characterization of orthorhombic $LaLuO_3$ using extreme ultraviolet reflectometry. *Thin Solid Films.* 2019. **680**: 94.

7. Danilov N., Vdovin G., Reznitskikh O., Medvedev D., Demin A., Tsiakaras P. Physico-chemical characterization and transport features of protonconducting Sr-doped $LaYO_3$ electrolyte ceramics. *J. Eur. Ceram. Soc.* 2016. **36**(11): 2795.
8. Sakai T., Isa K., Matsuka M., Kozai T., Okuyama Y., Ishihara T., Matsumoto H. Electrochemical hydrogen pumps using Ba doped $LaYbO_3$ type proton conducting electrolyte. *Int. J. Hydrogen Energy.* 2013. **38**(16): 6842.
9. Lesnichyova A., Stroeva A., Belyakov S., Farlenkov A., Shevyrev N., Plekhanov M., Khromushin I., Aksenova T., Ananyev M., Kuzmin A. Water uptake and transport properties of $La_{1-x}Ca_xScO_{3-\alpha}$ proton-conducting oxides. *Materials.* 2019. **12**(14): 2219.
10. Artini C., Costa G.A., Masini R. Study of the formation temperature of mixed $LaREO_3$ (RE: Dy, Ho, Er, Tm, Yb, Lu) and $NdGdO_3$ oxides. *J. Therm. Anal. Calorim.* 2011. **103**: 17.
11. Chudinovych O.V., Bykov O.I., Samelyuk A.V. Phase relation studies in the La_2O_3–Lu_2O_3–Yb_2O_3 system at 1500 °C. *J. Chem. Technol.* 2021. **29**(4): 485.
12. Chudinovych O., Bykov O., Samelyuk A. Interaction of Lanthanum, Lutetium, and Ytterbium Oxides at 1600 °C. *Powder Metall. Met. Ceram.* 2021. **60**: 337.
13. Kornienko O., Yushkevych S., Bykov O., Samelyuk A., Bataiev Y. Phase Equilibrium in the Ternary CeO_2–La_2O_3–Yb_2O_3 System at 1500 °C. *Solid State Phenomena.* 2022. **331**: 159.
14. Athayde D., Souza D.F., Silva A., Vasconcelos D., Nunes E.H., da Costa J.C.D., Vasconcelos W. Review of perovskite ceramic synthesis and membrane preparation methods. *Ceram. Int.* 2016. **42**(6): 6555.
15. Navas D., Fuentes S., Castro-Alvarez A., Chavez-Angel E. Review on Sol-Gel Synthesis of Perovskite and Oxide Nanomaterials. *Gels.* 2021. **7**(4): 275.
16. Sakka S. History of the Sol–Gel Chemistry and Technology. In: *Handbook of Sol-Gel Science and Technology.* (Berlin: Springer Cham, 2020).
17. Serivalsatit K., Wasanapiarnpong T., Kucera C., Ballato J. Synthesis of Er-doped Lu_2O_3 nanoparticles and transparent ceramics. *Opt. Mater.* 2013. **35**(7): 1426.
18. Salavati-Niasari M., Hosseinzadeh G., Davar F. Synthesis of lanthanum carbonate nanoparticles via sonochemical method for preparation of lanthanum hydroxide and lanthanum oxide nanoparticles. *J. Alloys Compd.* 2011. **509**(1): 134.
19. Mousavi-Kamazani M., Alizadeh S., Ansari F., Salavati-Niasari M. A controllable hydrothermal method to prepare $La(OH)_3$ nanorods using new precursors. *J. Rare Earths.* 2015. **33**(4): 425.
20. Nakamoto K. *Infrared and Raman spectra of inorganic and coordination compounds*: *Part A: Theory and Applications in Inorganic Chemistry*. (Wiley-Interscience: John Wiley & Sons, Inc., 2008).
21. Gregg S.J., Sing K.S.W. *Adsorption, Surface Area and Porosity*. (London: Academic Press, 1982).
22. Everett D.H. IUPAC Manual of Symbols and Terminology, Appendix 2, Pt. I, Colloid and Surface Chemistry. *Pure Appl. Chem.* 1972. **31**: 578.
23. Ragulya A.V., Baglej N.N., Lobunets T.F., Polotaj A.V., Klimenko V.P. Evolution of the structure of thermal decomposition products of barium titanyl oxalate crystalline hydrate under non-isothermal conditions. I. Nitrogen adsorption isotherms on decomposition products formed by low- and high-speed linear heating of barium titanyl oxalate. *Nanokristallicheskie materialy.* 2003. 39. [in Russian].
24. Ragulya A.V., Lobunets T.F., Baglej N.N., Polotaj A.V., Klimenko V.P. Evolution of the structure of thermal decomposition products of barium titanyl oxalate crystalline hydrate under non-isothermal conditions. II. Differential curves of pore size distribution in thermal decomposition products of barium titanyl oxalate. *Nanokristallicheskie materialy.* 2003. 43. [in Russian].
25. Gopalakrishnamurthy H.S., Subba Rao M., Narayanan Kutty T.R. Thermal decomposition of titanyl-oxalates. I. Barium titanyl-oxalate. *J. Inorg. Nucl. Chem.* 1975. **37**(4): 891.
26. Gablenz S., Abicht H.-P., Pippel E., Lichtenberger O., Woltersdorf J. New evidence for an oxycarbonate phase as an intermediate step in $BaTiO_3$ preparation. *J. Eur. Ceram. Soc.* 2000. **20**(8): 1053.
27. Duran P., Gutierrez D., Tartaj J., Banares M.A., Moure C. On the formation of an oxycarbonate intermediate phase in the synthesis of $BaTiO_3$ from (Ba,Ti)-polymeric organic precursors. *Ibid.* 2002. **22**(6): 797.

Received 27.02.2025, accepted 04.09.2025